AIAA JOURNAL
Vol. 40, No. 5, May 2002

Analysis and Testing of a Postbuckled Stiffened Panel

M. Lillico,* R. Butler,† and G. W. Hunt‡
University of Bath, Bath, England BA2 7AY, United Kingdom
and
A. Watson,§ D. Kennedy,¶ and F. W. Williams**
Cardiff University, Cardiff, Wales CF24 3TB, United Kingdom

The suitability of using the efficient, linear elastic design software VICONOPT for the analysis of a stiffened panel with a postbuckling reserve of strength is investigated. A longitudinally compressed panel, which initially buckled in a local skin mode, was analyzed with allowance being made for the effects of an initial overall imperfection. The panel was also analyzed using the nonlinear finite element package ABAQUS, and four laboratory specimens that represent the panel were tested to failure. The similarity of the experimental failure with the VICONOPT and ABAQUS predictions indicates that VICONOPT can give satisfactory analysis results for use in preliminary design.

I. Introduction

IT is well known[1] that stiffened panels can have a considerable postbuckling reserve of strength, enabling them to carry loads in excess of their initial buckling load when initial buckling is in a local mode, for example, skin buckling between stiffeners, but not if it is in an overall mode, for example, an Euler or wide column mode. The design of aerospace structures places great emphasis on mass minimization of such panels to reduce lifecycle costs. An optimum (minimum mass) design procedure based on initial buckling, stress, or strain, and stiffness constraints typically results in an idealized structural configuration that has almost equal critical loads for local and overall buckling, resulting in little postbuckling strength and a susceptibility to premature failure.[2] Recent techniques can produce lower mass designs for a given loading by permitting initial local buckling below the design load and allowing for the response characteristics known to exist in postbuckled plates.[3–5]

This paper presents an efficient method of analysis, suitable for the preliminary optimum design of a stiffened panel with a postbuckling reserve of strength, employing the industrially used linear elastic software VICONOPT.[6] The initial buckling mode is a local skin mode in longitudinal compression, and the panel is loaded beyond initial buckling to failure, with an allowance being made for the effects of an initial overall imperfection and a postbuckled neutral axis shift. The VICONOPT analysis involves calculating the change in stiffness of all plates following initial buckling and allows for the associated redistribution of stress between initial buckling and ultimate failure.

The panel has also been analyzed using the finite element package ABAQUS,[7] and four test specimens representing the panel have been fabricated and tested experimentally. The present paper compares the VICONOPT, ABAQUS, and experimental results, and thereby assesses the suitability of VICONOPT for analysis during preliminary design of a panel with a postbuckling reserve of strength.

Received 12 February 2000; presented as Paper 2000-1659 at the AIAA/ASME/ASCE/AHS/ASC 41st Structures, Structural Dynamics, and Materials Conference, Atlanta, GA, 3–6 April 2000; revision received 26 July 2001; accepted for publication 14 December 2001. Copyright © 2002 by the American Institute of Aeronautics and Astronautics, Inc. All rights reserved. Copies of this paper may be made for personal or internal use, on condition that the copier pay the $10.00 per-copy fee to the Copyright Clearance Center, Inc., 222 Rosewood Drive, Danvers, MA 01923; include the code 0001-1452/02 $10.00 in correspondence with the CCC.

*Research Assistant, Department of Mechanical Engineering; currently Professional Engineer, Airbus U.K., Filton, Bristol, England BS99 7AR, United Kingdom.
†Senior Lecturer in Aerospace Structures, Department of Mechanical Engineering.
‡Professor of Structural Mechanics, Department of Mechanical Engineering.
§Research Associate, Cardiff School of Engineering.
¶Senior Lecturer, Cardiff School of Engineering. Member AIAA.
**Professor of Structural Engineering, Cardiff School of Engineering.

II. VICONOPT: Design, Analysis, and Results

A. Example Panel

An earlier version[8] of VICONOPT containing an empirical postbuckling capability was used to produce the minimum mass design indicated in Fig. 1, with free longitudinal edges and simply supported transverse edges, subject to sets of buckling, material strength, and practical constraints. Aluminum 6082-T6 was used to fabricate the panels, with elastic modulus $E = 72.4$ GPa, Poisson's ratio $\nu = 0.33$, and the 0.2% proof stress = 283 MPa. The panel was designed to carry a compressive load of 69 kN applied at its neutral axis, with a maximum allowable midsurface strain (to at least stay close to the VICONOPT elastic assumptions) of 3600 microstrain in any plate. The panel design allowed for both positive and negative overall imperfections, varying in a half sine wave over the length of the panel such that the imperfection is zero at the ends and δ_0 throughout the midlength cross section, the positive direction for δ_0 being shown in Fig. 1. The magnitude of δ_0 was $l/500$, and the interstiffener portions of skin were designated to buckle initially at 60% of the design load, that is, at around 41 kN, with an empirically chosen postbuckled to prebuckled stiffness ratio of 0.5. This version of the program has since been extended to calculate the postbuckled stiffness of plates[9] and to allow for the boundary conditions associated with the experimental tests of Sec. IV. These theoretical extensions are now described in the context of the general VICONOPT analysis capability, before the analysis results obtained using these VICONOPT extensions for the example panel are presented.

B. VICONOPT Analysis

VICONOPT[6] is a FORTRAN 77 computer program that incorporates the earlier programs VIPASA and VICON. It covers prismatic plate assemblies, that is, panels of constant cross section, composed of anisotropic plates, each of which can carry any combination of uniformly distributed and longitudinally invariant in-plane stresses. It can be used as either an analysis or an optimum design program. The analysis principally covers the calculation of eigenvalues, that is, the critical load factors in elastic buckling problems or the natural frequencies in undamped vibration problems. The analysis is based on the exact solution of the governing differential equations of the constituent members, which are assumed to undergo a deformation that varies sinusoidally to infinity in the longitudinal direction, yielding exact stiffness matrices whose elements are transcendental functions of the load factor or frequency and the axial half-wavelength λ of the deformation. The resulting transcendental eigenproblem requires an iterative solution that is performed using the Wittrick–Williams algorithm.[10] The simplest form of the

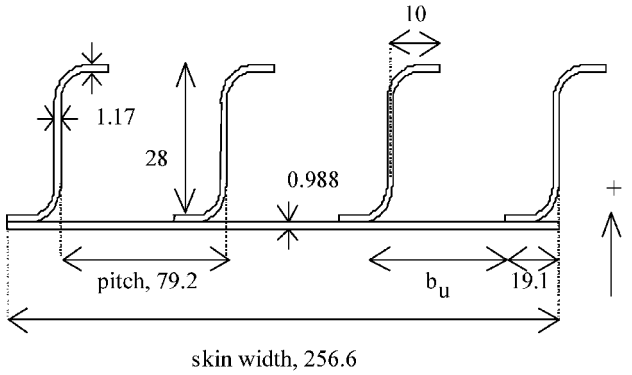

Fig. 1 Cross section of the example panel showing the direction taken as positive for the imperfection; all dimensions are in millimeters, the unsupported skin width b_u = 63.5 mm, and the panel length l was 539 mm.

buckling analysis[11,12] is performed over a range of values of λ that usually extends from a value less than the smallest plate width to the length l of the panel. The lowest buckling load found for any λ is taken as the critical buckling load for the panel. This implies that the panel of length l is simply supported at its ends with warping of the entire cross section allowed.

For panels with postbuckling strength, modifications were made to the basic method of VICONOPT. These and the original VICONOPT options are too extensive to quote in detail, and so only the features and options needed to understand the current paper are given here.

1. Approximate Postbuckling Stiffness Calculation

Local buckling loads and modes, considered to be at any $\lambda < l$, are first found. Then, for collapse, which may be due to overall or torsional (stiffener) buckling or material failure, the in-plane stiffnesses of the locally buckled plates are reduced by multiplying the prebuckled stiffnesses by a factor r_s that may be preselected by the user.[8] However, in this paper, a separate VICONOPT postbuckling analysis[9] was performed so that values of r_s were automatically calculated for each plate in the assembly. Each value of r_s is obtained by dividing the plate stiffness after buckling by its stiffness before buckling, where the plate stiffness is obtained by dividing the average axial stress in the plate by the total axial strain at the neutral axis of the panel. The axial strain in each plate has two components: one due to axial loading and one due to out of plane flexure. Because the total strain is assumed to be uniform across the panel width, those plates that have buckled most will have the greatest strain components due to flexure, the smallest strain components due to axial load, and, therefore, comparatively small components of axial stress, leading to low values of r_s.

When a plate is loaded axially and its longitudinal edges are required to remain straight, a nonuniform transverse stress distribution develops. This is composed of tension and compression regions, such that integration along the length gives a zero transverse stress resultant. Because the compression regions occur adjacent to the nodal lines, that is, lines of zero out-of-plane displacement, whereas tension regions occur around the midlength of each half-wavelength, the tension regions have a greater stabilizing effect than the destabilizing effects of the compression regions. This is allowed for in VICONOPT[9] by loading the plate with a uniform, that is, longitudinally invariant, transverse tension equal to some fraction τ of the maximum transverse tension calculated from the postbuckling mode. The value $\tau = 0.3$ was chosen for the present work, based on previous studies on stiffened panels,[8] although the effect of variation in τ is also considered in the results that follow.

The preceding modifications are clearly approximations to more rigorous approaches (such as Refs. 3 and 13) that use Koiter's postbuckling theory to account realistically for many of the actual characteristics known to exist in postbuckled plates. However, the method has been shown[9,14] to give good agreement with the results of these more rigorous approaches for compression-loaded plates and panels, and its use here for preliminary design is justified on the basis of these previous results and the results that follow.

2. Local/Overall Interaction

A further modification was to perform approximate calculations, based on an earlier method,[15] to allow for an overall imperfection of amplitude δ_0 and, as described in Ref. 14, to allow for the experimental boundary conditions in which a single-bay panel of length l is compression tested. Here, the end load position throughout the test remains along the unbuckled neutral axis, so that when the skin buckles the effective neutral axis position shifts away from the skin, causing an offset between the load and the buckled neutral axis.

Hence, by treating the entire cross section of Fig. 1 as that of a wide strut, a moment M is considered in addition to the compressive load P and assumed to act over the entire panel length during local buckling and stress analysis, where

$$M = P\delta \tag{1}$$

For loads below the skin buckling load P_{sk}, there is no offset, and the midlength deflection δ is given by the following well-known equation:

$$\delta = \delta_0/(1 - P/P_E) \tag{2}$$

where P_E is the Euler or overall buckling load of the unbuckled panel and δ_0 is the amplitude of the initial imperfection (see curve 1 of Fig. 2).

After the skin has buckled, that is, $P \geq P_{sk}$, the situation is more complex, and models can be developed to describe single- and multi-bay cases.[14] For the single-bay (experimental test) case considered here, where the load remains applied at the neutral axis of the original (unbuckled) panel, an offset e_{sk} is introduced to represent the offset associated with the load above P_{sk}. Hence, the midlength deflection δ is given by

$$\delta = \frac{\delta_{0,sk}}{1 - P/P_{E,sk}} + e_{sk}\left(1 - \frac{P_{sk}}{P}\right)\left[\sec\left(\frac{\pi}{2}\sqrt{\frac{P}{P_{E,sk}}}\right) - 1\right] \tag{3}$$

where $P_{E,sk}$ is the Euler or overall buckling load of the skin-buckled panel. Values of $P_{E,sk}$ and e_{sk} are calculated by assuming that the stiffness of the skin is reduced by applying the factor r_s following buckling. The effect of the offset e_{sk} is to increase the compression in the skin following buckling (see curve 2 of Fig. 2). The amplitude of the initial imperfection for the skin-buckled panel $\delta_{0,sk}$ is given by equating Eqs. (2) and (3) with $P = P_{sk}$. Hence,

$$\delta_{0,sk} = \delta_0/(1 - P_{sk}/P_E) \times (1 - P_{sk}/P_{E,sk}) \tag{4}$$

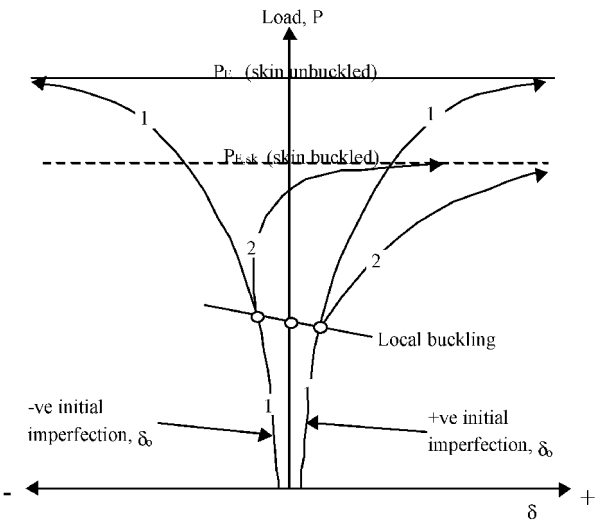

Fig. 2 Schematic representation of load vs midlength deflection for initial (prebuckling) panel (curve 1) and postbuckled panel (curve 2); P_E is the Euler or overall load of the panel and the hollow circles denote local skin buckling loads. [Note that positive (negative) δ increases (decreases) compression in the skin and decreases (increases) compression in the stiffeners.]

Table 1 Experimental results[a] and theoretical predictions[a]

	Experimental test									
Result	A	B	C	D	VICONOPT			ABAQUS		
Initial imperfection	+ve	+ve	+ve	−ve	$+l/500$	0	$-l/500$	$+l/500$	0	$-l/500$
Local buckling load, kN	37.0	37.0	41.0	46.0	39.6	43.6	49.3	39.1	40.8	45.9
Failure load kN,	72.0	71.6	74.0	77.0	68.1	77.6	95.9	65.4	70.8	78.8

[a]In all cases, local buckling occurred in the skin with nine half-wavelengths over the length of the panel and failure occurred as a result of a combined skin/overall mode of the type shown in Fig. 3.

Table 2 Peak centerline μ strain at 69 kN[a]

Imperfection	VICONOPT	ABAQUS
$+l/500$	−3712 (SK)	−5665 (SK)[b]
0	−2758 (SK)	−3565 (SK)
$-l/500$	−2546 (ST)	−2692 (SK)

[a]SK and ST denote skin and stiffener, respectively, and negative strain is compressive.
[b]Peak strain is given at 65.5 kN.

Table 3 Measured material properties for Al 6082-T6 used in the skin (SK) and stiffeners (ST)

SK/ST	Microstrain	0	2000	3000	4000	5000	6000
SK	σ, MPa	0	156	223	277	299	309
	E, GPa	76.1	72.5	66.6	36.4	12.8	6.4
ST	σ, MPa	0	154	220	266	286	294
	E, GPa	71.6	69.5	60.8	26.5	12.4	4.4

For the results that follow, the values for P_E and $P_{E,\mathrm{sk}}$ were overall panel buckling loads calculated by VICONOPT, rather than Euler loads.

C. VICONOPT Results

The VICONOPT analysis used an infinitely wide model for the panel of Fig. 1, based on a repeating portion comprising one stiffener and associated skin of width 79.2 mm. The initial buckling and failure modes were found to repeat over two such repeating portions. As can be seen in Fig. 1, the flanges at either end of the stiffener include curved portions. These were each modeled using five flat plates, to approximate a circular arc with a centerline radius of 3 mm. The model allowed for the offsets[11] between the centerlines of connected plates. The lower flange and the associated skin were modeled as a single plate, representing perfect adhesion between them. To model the stress distribution after initial buckling, each plate was divided into four strips of equal width, each carrying a different, longitudinally invariant, stress. The aluminum was assumed to be linear elastic with modulus $E = 72.4$ GPa and Poisson's ratio $\nu = 0.33$.

The VICONOPT initial buckling and failure loads of the perfect and imperfect panels are given in Table 1. For the positive imperfection the failure load is 68.1 kN, whereas for the negative imperfection the failure load is some 40% higher. The critical half-wavelength for initial buckling is $l/9 = 59.9$ mm, that is, approximately equal to the width of the interstiffener portion of skin. The peak strains at the original design load (69 kN) are given in Table 2. These strains are centerline strains in the respective plates. They occurred in the skin for the positive imperfection case and in the remote flange for the negative imperfection case. Failure in all cases was precipitated by material yield in the skin (i.e., when the strain in the skin exceeded 3600 microstrain) and would be in the form of a combined skin/overall mode. Additional runs for the negative imperfection case showed that the failure load was decreased by less than 7% when the transverse tension factor τ was reduced from 0.3 to the more conservative value of 0.1.

III. ABAQUS: Modeling and Results

A. ABAQUS Model

Finite element (FE) modeling was carried out to determine both the bifurcation buckling and the postbuckling behavior of the panel, using the package ABAQUS.[7] The purpose was both to validate the VICONOPT analysis and to predict the failure of an actual panel in the laboratory. The model used 10160 Quad 4 thin shell elements. The simply supported end conditions and load distribution were applied such that the load remained along the neutral axis of the unbuckled panel both before and after the onset of buckling. A simple check was carried out to confirm these boundary conditions by ensuring that uniform axial strain was obtained before buckling when no imperfection was present. The effect of material plasticity was included using the material properties given in Table 3 and

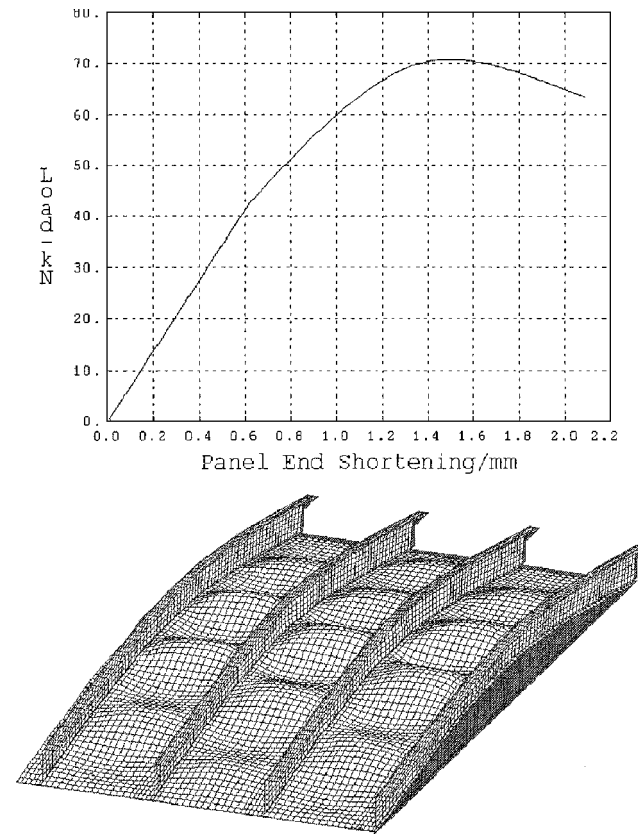

Fig. 3 End shortening plot and final deformed shape given by the ABAQUS model for the perfect panel.

$\nu = 0.33$. These properties were obtained from a series of tensile tests on samples of the material.

B. ABAQUS Results

Table 1 shows that there is agreement of 7% or better between the local buckling loads given by ABAQUS and those given by VICONOPT. The ABAQUS solutions are lower, due to the effects of accounting for the nonlinear material behavior. (ABAQUS linear bifurcation analysis gave a local buckling load of 43.8 kN for the perfect panel.) They are also more approximate than the VICONOPT results because they were obtained from nonlinear analysis either by checking for negative eigenvalues at each analysis step, or, in the case of the negative imperfection result, by observing a stiffness change in the load end shortening relationship. In all cases, the buckling is in the form of a skin mode with nine half-wavelengths over the panel length.

Table 1 also compares the nonlinear failure solutions found using ABAQUS and VICONOPT, and Fig. 3 shows a typical ABAQUS

end shortening plot and deformed shape just before collapse for the perfect panel. ABAQUS predicts that for the $+l/500$ case the panel will not quite be able to support the original design load of 69 kN. This is due to the effects of plasticity (see following discussion). However, for both the negative and zero imperfection cases, the model predicts that the panel will satisfy the design load requirement. For all FE solutions the predicted failure mode is an interaction between a skin mode with nine half-wavelengths and an overall mode.

The ABAQUS peak strains at a load of 69 kN, given in Table 2, all occur in the skin, next to the stiffener, on the side opposite the lower flange. For the perfect panel, the level of strain is close to the point were the material starts to behave plastically. This explains why in the ABAQUS solution for the $+l/500$ case the panel fails at a load of 65.5 kN, at which the peak strain is well into the region where the material behaves plastically.

IV. Experimental Testing and Results

A. Experimental Procedure

Four panels were manufactured to the design of Fig. 1. Stiffeners were attached to the skin using adhesive plus a single row of rivets that were placed at 25 mm spacing along the middle of the stiffener lower flanges. Once the stiffeners had been attached, the panel ends were machined to ensure that they were flush. The experimental methodology has previously been used successfully.[16] For the current set of tests, strains before and after initial buckling were recorded using strain gauges attached across the midlength of the panel to each stiffener upper flange, the middle of each skin section, and to the lower web of the two central stiffeners. The recorded strains were compared to prebuckling predictions of strain in the panel, to both monitor the test imperfections, ensuring that they were within acceptable limits, and also to help determine the onset and advance of buckling. For brevity, only a representative sample of the strain data will be presented.

B. Experimental Results

The experimental results obtained during the laboratory tests are compared with the predictions given by VICONOPT and ABAQUS in Table 1. With the exception of the negative imperfection result, there is good agreement between the predicted and experimental failure loads. All of the panels failed at loads greater than the original design load despite the initial imperfection being in the weaker positive direction for tests A–C. The cause of failure for two experiments differs from that predicted by theoretical methods. ABAQUS predicted that, in every case, failure is due to an interaction between the initial skin mode and an overall mode. In tests A and B failure was due to a localized buckle in the lower flange/skin interface at the free panel edge (Fig. 4). Some plastic deformation in the skin sections also occurred across the panel, originating from the large plastic deformation at the panel edge. In tests C and D (Fig. 4), the predicted type of failure occurred. In every case, the panel retained the ability to carry load after failure, although the load dropoff varied between 14% of the failure load for the test A and 68% for test D.

The local buckling loads were assumed to occur when the strain–load relationship ceased to be linear. In Fig. 5, which shows the strain at the midbreadth of the central skin section during test B, this point can clearly be seen. Here, SK2 is the strain gauge attached to the surface of the central skin section at the panel midlength, on the side of the stiffeners, whereas SK2R is the strain gauge directly opposite on the other side of the skin and is visible in the test B photograph of Fig. 4. Figure 6 shows the similarity in ABAQUS prediction of strain at this point in the skin but indicates initial local buckling in the opposite sense to the experimental data given in Fig. 5. This difference is a consequence of the multiple equilibrium states following bifurcation buckling.

The local buckling loads of panel tests A and B were about 5.4% (6.6%) below the lowest value predicted by the ABAQUS (VICONOPT) model, whereas the loads given by tests C and D were within the range of the predicted values for both models. The local buckling load for test D was the highest due to the negative initial imperfection. The differences between the values given for tests A, B, and C may partly be because the stiffeners in test C were made from a different sheet of Al6082-T6 from that used for the stiffeners for tests A and B and also because the initial imperfection was bigger in tests A and B. In all of the laboratory tests, the panels initially buckled in the skin, in nine half-wavelengths, and remained buckled in this state until failure. This matches both the ABAQUS

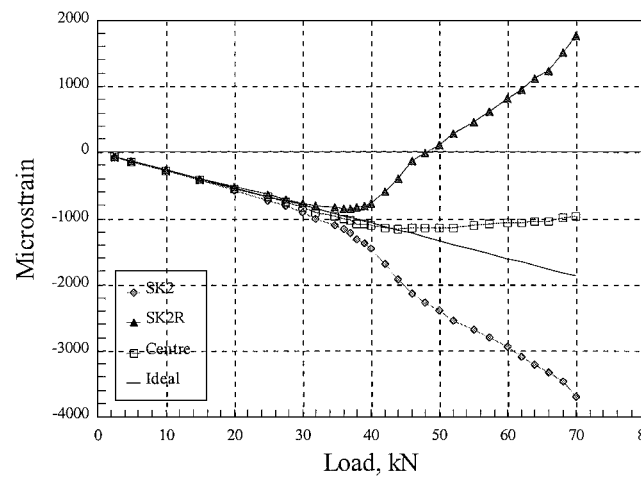

Fig. 5 Strain at the midlength of the central skin section during test B.

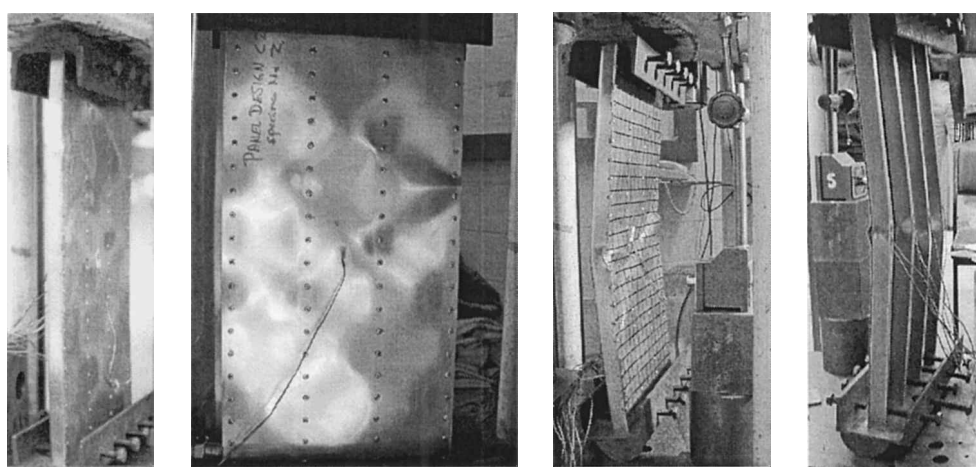

Fig. 4 Panel failure modes: in tests A and B panel failure were due to localized buckling at the panel edge, whereas in tests C and D failures were due to interaction between skin and overall modes.

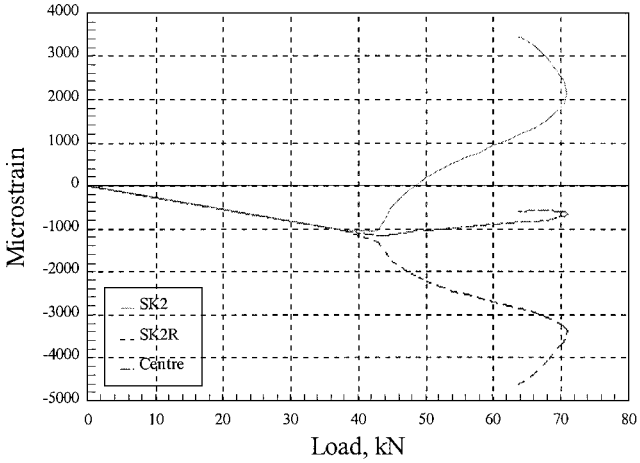

Fig. 6 ABAQUS strain at the midlength of the central skin section for the perfect panel.

and VICONOPT buckled shape predictions. However, there is evidence in the strain data taken during test A to suggest that a change in the buckling pattern occurred. It is thought that the length of each half-wavelength was not uniform along the panel and changed as load was applied.

V. Discussion

The solutions obtained by VICONOPT are not the result of a fully nonlinear analysis, but of an approximate analysis of the panel in its assumed buckled state. However, as can be seen from the results given, VICONOPT predicted that the panel would initially buckle in the skin and then behave in a stable manner in the postbuckled regime. This behavior was confirmed by the nonlinear ABAQUS model and by the tests carried out in the laboratory. The VICONOPT results were obtained using 56 strip elements compared to the 10,000 or more shell elements in the ABAQUS results.

With the exception of the positive imperfection models, for which failure occurred at 95 and 99% of the original design load, the ABAQUS and VICONOPT models predicted that the design would carry the design load and that failure would be in a combined skin/overall mode. For the theoretical cases, initial buckling loads for positive and negative imperfections agreed to within 2 and 7%, respectively, and failure loads to within 4 and 18%, respectively. The VICONOPT loads are consistently higher than those given by ABAQUS, due to the effects of accounting for plasticity in the ABAQUS model. With the exception of the local buckling loads for tests A and B, the experimental loads all lie within the range of the theoretically predicted loads, suggesting that the actual imperfections were less than those modeled.

The strains predicted by VICONOPT at the design load of 69 kN are consistently lower than those predicted by ABAQUS. The main reason for this is that the VICONOPT analysis is based on linear elastic theory, whereas Tables 2 and 3 confirm that, in the ABAQUS analysis, some plates were already behaving plastically at the design load. In addition, VICONOPT only gives an average value for the peak strain in the skin, whereas ABAQUS takes into account the variation in strain distribution caused by the actual postbuckled shape of the panel. Note that, for the negative imperfection case, the VICONOPT peak strain is in the remote stiffener flange, indicating that, at this level of load, the influence of the offset in Eq. (3) is not sufficient to produce postive central deflection (see Fig. 2).

In all cases, the panel is initially loaded along its unbuckled neutral axis. When the skin buckles, the neutral axis moves away from the skin, but the load position remains fixed, so that in the postbuckled regime there is an offset between the load and the neutral axis. This results in an out-of-plane bending moment, which exaggerates the skin buckling, causing failure on the skin side, even when the initial imperfection is negative and initially increases compression in the stiffener (see Fig. 2). Note that an earlier study[14] has shown that the VICONOPT model can be adapted so that the load follows the shift in the neutral axis position after buckling. This so-called multibay model matches the boundary conditions in a compression panel of an actual aircraft wing subject to overall bending moment.

VI. Conclusions

The local buckling loads, failure loads, and buckled mode shapes given by both the linear elastic VICONOPT model and the plastic ABAQUS model match well with the behavior of the panel in the laboratory. The VICONOPT results, though approximate, require a fraction of the computational effort required by the ABAQUS runs. Hence, the paper indicates that VICONOPT can give satisfactory analysis results for use in preliminary design of postbuckled compression panels assuming linear elastic material properties.

Acknowledgments

The authors wish to thank the Engineering and Physical Sciences Research Council (GR/M26220 and GR/M26237) and Airbus U.K. for providing the financial assistance that made this work possible. In addition they would like to thank M. S. Anderson for the helpful comments he has made.

References

[1]Hutchinson, J. W., and Koiter, W. T., "Postbuckling Theory," *Applied Mechanics Reviews*, Vol. 23, Dec. 1970, pp. 1353–1366.

[2]Hunt, G. W., "An Algorithm for the Non-Linear Analysis of Compound Branching," *Philosophical Transactions of the Royal Society of London*, Vol. A300, No. 1455, 1981, pp. 443–471.

[3]Bushnell, D., "Optimization of Composite, Stiffened, Imperfect Panels Under Combined Loads for Service in the Postbuckling Regime," *Computer Methods in Applied Mechanics and Engineering*, Vol. 103, Nos. 1–2, 1993, pp. 43–114.

[4]Bushnell, D., Rankin, C. C., and Riks, E., "Optimization of Stiffened Panels in Which Mode Jumping is Accounted For," *Proceedings of 38th AIAA/ASME/ASCE/AHS/ASC Structures, Structural Dynamics, and Materials Conference*, AIAA, Reston, VA, 1997, pp. 2123–2162.

[5]Everall, P. R., and Hunt, G. W., "Arnold Tongue Predictions of Secondary Buckling in Thin Elastic Plates," *Journal of the Mechanics and Physics of Solids*, Vol. 47, No. 10, 1999, pp. 2187–2206.

[6]Williams, F. W., Kennedy, D., Butler, R., and Anderson, M. S., "VICONOPT: Program for Exact Vibration and Buckling Analysis or Design of Prismatic Plate Assemblies," *AIAA Journal*, Vol. 29, No. 11, 1991, pp. 1927, 1928.

[7]"ABAQUS/Standard User's Manual," Ver. 5.7, Hibbitt, Karlsson, and Sorensen, Inc., Pawtucket, RI, 1997.

[8]Anderson, M. S., "Design of Panels Having Postbuckling Strength," *Proceedings of 38th AIAA/ASME/ASCE/AHS/ASC Structures, Structural Dynamics, and Materials Conference*, AIAA, Reston, VA, 1997, pp. 2407–2413.

[9]Powell, S. M., Williams, F. W., Askar, A.-S., and Kennedy, D., "Local Postbuckling Analysis for Perfect and Imperfect Longitudinally Compressed Plates and Panels," *Proceedings of 39th AIAA/ASME/ASCE/AHS/ASC Structures, Structural Dynamics, and Materials Conference*, AIAA, Reston, VA, 1998, pp. 595–603.

[10]Wittrick, W. H., and Williams, F. W., "A General Algorithm for Computing Natural Frequencies of Elastic Structures," *Quarterly Journal of Mechanics and Applied Mathematics*, Vol. 24, Pt. 3, 1971, pp. 263–284.

[11]Wittrick, W. H., and Williams, F. W., "Buckling and Vibration of Anisotropic or Isotropic Plate Assemblies Under Combined Loadings," *International Journal of Mechanical Sciences*, Vol. 16, No. 4, 1974, pp. 209–239.

[12]Anderson, M. S., Williams, F. W., and Wright, C. J., "Buckling and Vibration of Any Prismatic Assembly of Shear and Compression Loaded Anisotropic Plates with an Arbitrary Supporting Structure," *International Journal of Mechanical Sciences*, Vol. 25, No. 8, 1983, pp. 585–596.

[13]Dickson, J. N., and Biggers, S. B., "POSTOP: Postbuckled Open-Stiffener Optimum Panels—Theory and Capability," NASA CR-172259, Jan. 1984.

[14]Lillico, M., Butler, R., Hunt, G. W., Watson, A., and Kennedy, D., "Post Buckling of Single and Multibay Panels Using Strut, Strip, and Finite Element Methods," AIAA Paper 2001-1329, 2001.

[15]Anderson, M. S., and Stroud, W. J., "General Panel Sizing Computer Code and Its Application to Composite Structural Panels," *AIAA Journal*, Vol. 17, No. 8, 1979, pp. 892–897.

[16]Butler, R., Lillico, M., Hunt, G. W., and McDonald, N. J., "Experiments on Interactive Buckling in Optimized Stiffened Panels," *Structural and Multidisciplinary Optimization*, Vol. 23, No. 1, 2001, pp. 40–48.

E. R. Johnson
Associate Editor